Journal of Sound and Vibration (2002) **253**(5), 1087–1100
doi:10.1006/jsvi.2001.4085, available online at http://www.idealibrary.com on IDEAL®

VIBRATION SIGNAL ANALYSIS AND FEATURE EXTRACTION BASED ON REASSIGNED WAVELET SCALOGRAM

Z. Peng, F. Chu and Y. He

Department of Precision Instruments, Tsinghua University, Beijing 100084, *People's Republic of China*

(*Received* 10 *May* 2001, *and in final form* 23 *October* 2001)

The wavelet scalogram has been widely used for vibration signal analysis, but it has low frequency concentration at small scales and low time concentration at large scales owing to the limitation of Heisenberg–Gabor inequality. In addition, misleading interference terms would appear in the scalogram at some conditions. All of these would influence scalogram analysis seriously. In this paper, a reassignment method is used, which can improve the concentration of the scalogram and weaken the interference terms to a certain extent; thus, the readability of the scalogram can be improved. The experimental data for three kinds of faults in rotating machinery: rotor-to-stator rub, oil whirl, coupling misalignment and the actual measurement data from a Pumped Storage Power Generator Unit are analyzed by the scalogram and the reassigned scalogram, and the results by FFT analysis are also given. A comparison among three kinds of analysis results is carried out, and the comparison results indicate that the scalogram can not only reveal the time–frequency features of vibration signal but also highlight the components of low energy. Therefore, it is suitable to extract features of faults at an early stage.

1. INTRODUCTION

Fault diagnostics is useful for ensuring the safe running of rotating machines, and vibration signal analysis has been widely used for fault diagnostics. The key problem is how to extract useful features from vibration signals for fault diagnostics. Among many signal analysis methods, the FFT is one of the most widely used and well-established methods. Unfortunately, FFT-based methods are not suitable for non-stationary signal analysis and are not able to reveal the inherent information of non-stationary signals. However, various kinds of factors, such as the change of the environment and the faults from the machine itself, often make the vibration signal of the running machine contain non-stationary components. Usually, these non-stationary components have abundant fault information, so it is important to analyze the non-stationary signal [1]. Because of the disadvantages of the FFT, it is necessary to find supplementary methods for vibration signal analysis.

Hitherto, time–frequency analysis is the most popular method for the analysis of non-stationary vibration signals, such as the Gabor transform [2] (windowed Fourier transform), and the bilinear time–frequency representation [3]. They perform a mapping of one-dimensional signal $x(t)$ to a two-dimensional function of time and frequency $TFR(x{:}t, \omega)$. But all of the time–frequency analysis methods have disadvantages. For the Gabor transform, the limitation of Heisenberg–Gabor inequality makes the tradeoff between time and spectral resolutions unavoidable, and good time and spectral concentration cannot be obtained together in the time–frequency plane. Moreover, the

0022-460X/02/$35.00

spectrum of the Gabor transform is only a biased estimator of the instantaneous frequency and group delay of the signal. Bilinear time–frequency representations, such as the Wigner–Ville distribution and Margenau–Hill distribution have good concentration in the time–frequency plane. However, when support areas of the signal overlap each other, interference terms will appear on time–frequency plane. All the disadvantages mentioned above will mislead signal analysis. In order to overcome these disadvantages, many methods for improvement have been proposed. Without exception, however, elimination of one shortcoming will always lead to the loss of other merits. For example, the reduction of intereference terms will bring the loss of time–frequency concentration [4].

Over the past 10 years, wavelet theory [5] has become one of the emerging and fast-evolving mathematical and signal processing tools for its many distinct merits. Different from the Gabor transform, the wavelet transform (WT) can be used for multi-scale analysis of a signal through dilation and translation, so it can extract time–frequency features of a signal effectively. In the field of mechanical signal processing, the WT has been used for singularity detection [6], noise reduction [7] and feature extraction [8]. In addition, wavelet scalograms, the same as spectrums of the Gabor transform, are often used to analyze non-stationary signals and to extract time–frequency features of signals for fault diagnostics [9]. But the scalogram is also limited by the Heisenberg–Gabor inequality, so it is hard to obtain a good time and spectral concentration together in the time-scale plane. This shortcoming reduces the readability of the scalogram to a certain extent. In this paper, a reassignment method is applied to overcome this shortcoming and to improve the concentration in the time–frequency plane. Using the reassigned scalogram, a good discrimination of a signal's patterns can be obtained and signal classification can be achieved [10].

2. CONTINUOUS WAVELET TRANSFORM [5]

Assume $x(t)$ to be a finite-energy function, that is, $x(t) \in L^2(R)$. The continuous wavelet transform of $x(t)$ is defined as the inner product in the Hilbert space of the L^2 norm as follows:

$$W_x(a, b; \psi) = \langle x(t), \psi_{a,b}(t) \rangle = a^{-1/2} \int_{-\infty}^{+\infty} x(t) \psi^*_{a,b}(t)\, \mathrm{d}t \;\; a > 0, \tag{1}$$

where the asterisk stands for complex conjugate and the family of wavelet $\psi_{a,b}(t)$ consists of a series of son wavelets, which are generated by dilation and translation from the mother wavelet $\psi(t)$, as shown in the following:

$$\psi_{a,b}(t) = a^{-1/2} \psi\left(\frac{t-b}{a}\right), \tag{2}$$

where a is the scale parameter, b is the time parameter, and both of them vary continuously; the factor $a^{-1/2}$ is used to ensure energy preservation for transform. Many functions can be used as the mother wavelet, but it must belong to $L^2(R)$ and satisfy the following conditions:

1. The definition domain is compact support, which ensures that the function is fast decaying, and so time localization can be obtained.
2. The admissibility condition

$$C_\psi = \int \frac{|\hat{\psi}(\omega)|^2}{|\omega|} \mathrm{d}\omega < \infty, \tag{3}$$

where $\hat{\psi}(\omega) = \int \psi(t) e^{-iwt}\, dt$. This condition makes that the waveform of the mother wavelet function must be oscillating.

The wavelet transform is a linear transform, whose physical pattern is to use a series of oscillating functions with different frequencies as window functions $\psi_{a,b}(t)$ to scan and translate the signal of $x(t)$, where a is the dilation parameter for changing the oscillating frequency. Although the wavelet transform is similar to the Gabor transform in a certain sense, differences between them exist. Compared with the Gabor transform, whose time–frequency resolution is constant, the time–frequency resolution of the wavelet transform depends on the frequency of the signal. At high frequencies, the wavelet reaches a high time resolution but a low frequency resolution. At low frequencies, high frequency resolution and low time resolution can be obtained.

3. WAVELET SCALOGRAM [5]

For all $\psi(t)$, $x(t) \in L^2(R)$, the inverse wavelet transform of $x(t)$ is defined as

$$x(t) = \frac{1}{C_\psi} \int\int a^{-2} W_x(a, b; \psi) \psi_{a,b}(t)\, da\, db. \tag{4}$$

It can be shown from equation (4) that the wavelet transform does not lose any information, and the energy is preservative for the transform. So the following equation is tenable:

$$\langle x(t), x(t) \rangle = \int |x(t)|^2\, dt = \frac{1}{C_\psi} \int a^{-2}\, da \int |W_x(a, b; \psi)|^2\, db. \tag{5}$$

Owing to the limitation of the Heisenberg–Gabor inequality, there is no reason to think of $|W_x(a, b; \psi)|^2 / C_\psi a^2$ as the exact energy quantity at a point of the time-scale plane (a, b), but according to equality (5), it can be considered as the energy density function of the time-scale plane (a, b). It means that the $|W_x(a, b; \psi)|^2\ \Delta a \Delta b / C_\psi a^2$ represents the total energy of a domain centered at (a, b) with scale interval Δa and time interval Δb. Similar to the spectrum of the Gabor transform, $SG_x(a, b; \psi) = |W_x(a, b; \psi)|^2$ is defined as the wavelet scalogram. The wavelet scalogram has been widely used for the analysis of non-stationary signal, and the scalogram can be seen as a spectrum with constant relative bandwidth.

In every case, time and frequency resolutions of the scalogram are still bounded by the Heisenberg–Gabor inequality, and therefore cannot be both taken as small as desired.

4. THE REASSIGNMENT METHOD OF THE SCALOGRAM [10]

The reassignment method of the wavelet scalogram, which was derived from the spectrum reassignment method [11], was put forward by Francois Auger and Patrick Flandrin [10, 12]. Just as stated above, $|W_x(a_i, b_i; \psi)|^2$ cannot be seen as the energy of one point on the plane (a, b), and it represents the average of energy located in a domain with the geometrical center being $(\omega_0/a_i, a_i t^* + b_i)$. In the domain, however, the energy distribution is often not geometrically symmetrical, so it is not suitable to assign the average value to the geometrical center but to the point $(\omega_0/\hat{a}_i, \hat{a}_i t^* + \hat{b}_i)$, which is the gravity center of these energy contributions. As shown in Figure 1, the gravity center can better represent the energy distribution of the domain.

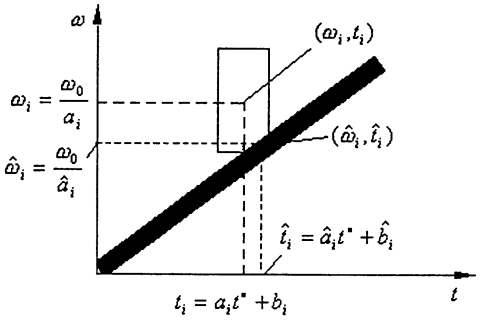

Figure 1. Energy distribution of linear frequency-modulated signal.

Figure 1 shows roughly the time-frequency distribution of energy of a linear frequency modulation signal, and the rectangle is a resolution window [5] determined by (a_i, b_i), whose height and width are the inverse ratio and direct ratio of a_i, respectively, and whose geometrical center is $(\omega_0/a_i, a_i t^* + b_i)$. $|W_x(a_i, b_i; \psi)|^2$ represents the average energy of the resolution window, but there is no energy at the geometrical center actually. Obviously, this averaging will lead to interference terms and poor concentration; and the higher the resolution window is, the lower the frequency concentration; the wider the resolution window is, the lower the time concentration. That is the reason why for the scalogram, the frequency concentration for a high frequency is lower than that for a low frequency. One way to avoid this is to change the contribution point of this average and reassign it to the center $(\omega_0/\hat{a}_i, \hat{a}_i t^* + \hat{b}_i)$ of the gravity of these energy distributions. The reassignment method of scalogram is a method to achieve this purpose. The reassignment method can improve the time and frequency concentrations of the scalogram, and so some low-energy components can be highlighted on the reassigned scalogram. Here the reassignment arithmetic is given, and the detailed information about the scalogram reassignment method can be found in reference [10].

The reassigned scalogram is defined by

$$RSG_x(\hat{a}, \hat{b}; \psi) = \int\int (\hat{a}/a)^2 SG_x(a, b; \psi)\delta(\hat{b} - b'(a, b))\delta(\hat{a} - a'(a, b))\,\mathrm{d}a\,\mathrm{d}b, \tag{6}$$

where

$$b'(a, b) = b - \mathrm{Re}\left\{a\frac{W_x(a, b; \psi')W_x^*(a, b; \psi)}{|W_x(a, b; \psi)|^2}\right\}, \tag{7}$$

$$\frac{\omega_0}{a'(a, b)} = \frac{\omega_0}{a} + \mathrm{Im}\left\{\frac{W_x(a, b; \hat{\psi})W_x^*(a, b; \psi)}{2\pi a|W_x(a, b; \psi)|^2}\right\}, \tag{8}$$

$$\psi'(t) = t\psi(t), \qquad \hat{\psi}(t) = \frac{\mathrm{d}\psi}{\mathrm{d}t}(t). \tag{9}$$

5. NUMERICAL EXPERIMENT

In order to illustrate the characteristics of the scalogram and the reassigned scalogram, a signal $x(t)$ will be considered. Figure 2 shows the signal $x(t)$ in the time domain and it can

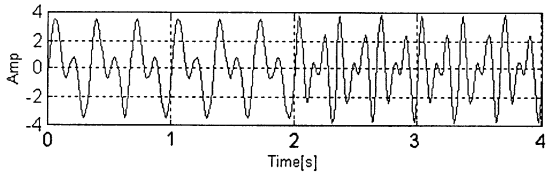

Figure 2. Numerical test signal $x(t)$.

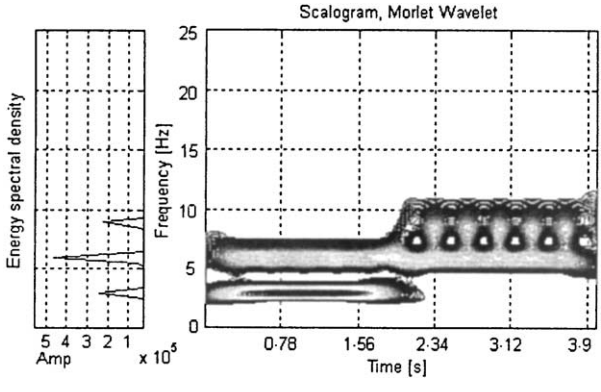

Figure 3. Spectrum and scalogram of $x(t)$.

be expressed by

$$x(t) = \begin{cases} 2\sin(6\pi t) + 2\sin(12\pi t), & 0 \leqslant t < 2 \text{ s}, \\ 2\sin(12\pi t) + 2\sin(18\pi t), & 2 \leqslant t \leqslant 4 \text{ s}. \end{cases} \tag{10}$$

The Morlet wavelet was used. The Morlet mother wavelet is defined by

$$\psi(t) = \pi^{-1/4} \mathrm{e}^{-\mathrm{i}\omega_0 t} \mathrm{e}^{-t^2/2}, \quad \omega_0 \geqslant 5. \tag{11}$$

Figure 3 is the scalogram of $x(t)$. In order to make a comparison with the spectrum, a conversion from scale to central frequency is made. This conversion is reasonable because every wavelet is a band-pass filter actually. The conversion can be expressed as

$$\omega = \omega_0 / a. \tag{12}$$

Although we know that the signal $x(t)$ contains three components whose frequencies are 3, 6 and 9 Hz, respectively, from the spectrum (left side of Figure 3), we cannot determine whether the component exists during all the signal's lifespan or only part of the lifespan. However, through the signal's scalogram, we are not only able to recognize, though not clearly, the three components but also able to know the time at which they exist. It is obvious that the concentration of the high frequency (small scale) is lower than that of the low frequency (big scale). Moreover, interference terms emerge at $2 \leqslant t \leqslant 4$ s in the scalogram but there are no interference terms at $0 \leqslant t < 2$ s, even though the frequency differences of the two components are the same at the two time regions. This is because the frequencies of the three components are close and the frequency concentration of the component with frequency $\omega = 9$ Hz is lower than that of the component with frequency $\omega = 3$ Hz. All of these bring obstacles for signal analysis.

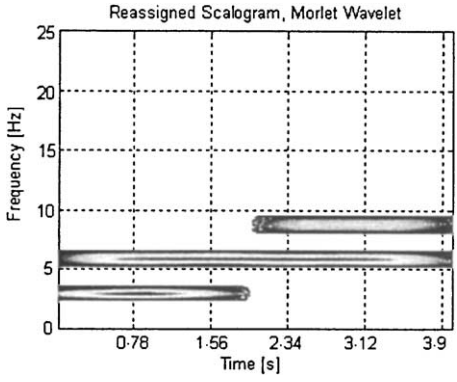

Figure 4. Reassigned scalogram of $x(t)$.

Figure 4 shows the reassigned scalogram of the signal $x(t)$. Obviously, the time and frequency concentrations are improved while the interference terms are reduced. Three components of signal $x(t)$ can be recognized clearly through the reassigned scalogram. The result shows that the reassignment method can improve the readability of a scalogram, which means both good concentrations of the signal components and no misleading interference terms.

Because of good concentration of the signal components, the reassigned scalogram can highlight components of low energy, so it can be used as a useful tool for extracting features of faults at their early stage. In the next section, the scalogram is used to analyze experimental data for three typical faults of rotating machines: rotor-to-stator rub, oil whirl, coupling misalignment.

6. EXPERIMENTAL DATA ANALYSIS [13]

Spectrum analysis plays an important role in fault diagnostics of rotating machines, and all faults have corresponding spectral features. During the early developing stage of a fault, however, those features are feeble and often submerged by the noise signal. Therefore, these fault features cannot be recognized clearly from the spectrum. This shortcoming bring some troubles for fault diagnostics at early stage. The scalogram can provide the time–frequency features of a signal, and the components with low energy can be shown clearly on the reassigned scalogram because the scalogram has a good concentration of the signal components. Therefore, the scalogram is a useful supplementary method for fault diagnostics at the early developing stage. In this section, the scalogram and the reassigned scalogram are used to analyze the experimental data of three typical faults in rotating machines: rotor-to-stator rub, oil whirl, coupling misalignment. Figure 5 shows the experimental test rig, which is mainly composed of rotors, a driving motor, journal bearings and couplings. Both vertical and horizontal vibration signals were picked up by non-contact eddy current transducers.

6.1. ROTOR-TO-STATOR RUB-IMPACT [14]

For rotating machines, rub-impact between rotor and stator is a kind of serious malfunction, which often happens at the positions with small clearances. This fault presents

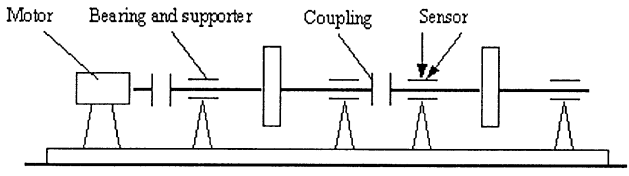

Figure 5. Experimental test rig.

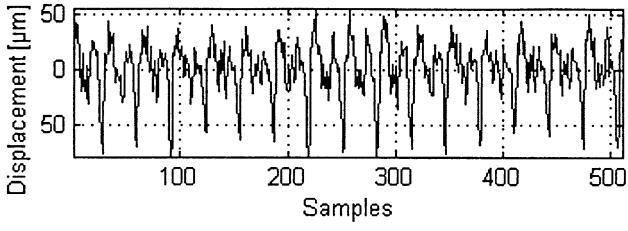

Figure 6. Rub-impact signal.

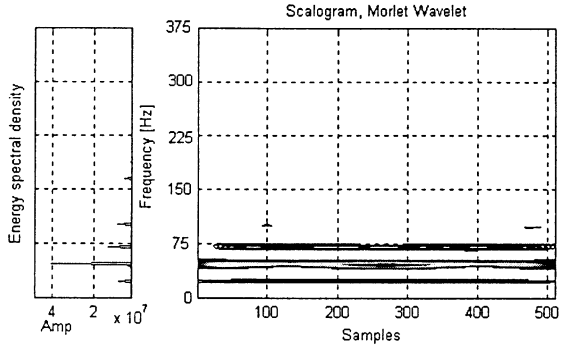

Figure 7. Spectrum and scalogram of rub-impact signal.

a serious hazard to machines. For example, the rub-impact between blades and seals would make the blade break down. The factors that influence rub-impact between rotor and stator are complicated, and the vibration phenomenon of a rub-impact rotor system is also complicated. A rub fault will cause not only periodic motions but also quasi-periodic motions. The way to extract useful features from vibration signals for diagnostics is still a problem under investigation. The scalogram is used to analyze the experimental data of rub-impact in this section.

The radial rub-impact between the rotor and stator is achieved by using a copper block to contact with rotor manually. Figure 6 shows a set of horizontal vibration data, which were sampled at a speed of 1·6 kHz. The rotary speed is 3000 r.p.m.

The left side of Figure 7 is the spectrum of the rotor-to-stator rub signal, through which it can be seen that the rub-impact fault excites the components of 1/2X, 1X, 3/2X, 2X, 3X, etc. It is obvious that the energy of signal mainly centralizes at 1X component, while other components are small and are not shown clearly in the spectrum. Compared with the spectrum, the scalogram (right side of Figure 7) shows all components clearly, and the approximate time for the appearance of components is also shown. But there are still some components not appearing on the scalogram, such as 3X component. It is just because that those components are of low energy and locate at high-frequency part where the frequency

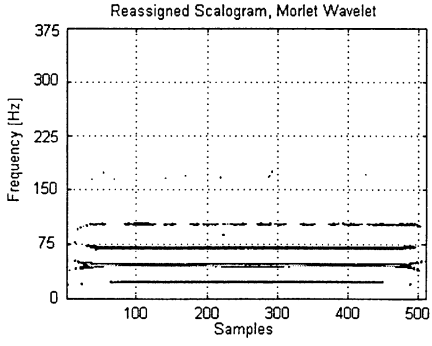

Figure 8. Reassigned scalogram of rub-impact signal.

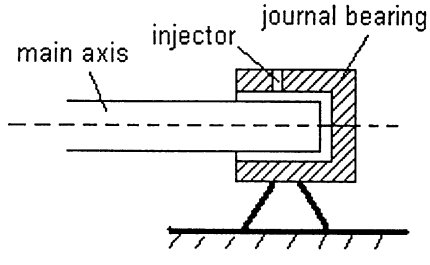

Figure 9. Simulating oil whirl.

concentration is low. Figure 8 is the reassigned scalogram whose concentration of signal components is better than the scalogram's. Through the reassigned scalogram, we can see the 3X component and can know that the 3X component does not exist continuously and has very low energy. The energy density is represented by different shades of the color. In addition, 2X component can be seen clearly. The comparison result indicates that the reassigned scalogram can reflect the inherent features of the rub-impact signal and can provide information for rub-impact machines analysis and more useful features for fault diagnostics.

6.2. OIL WHIRL

For a rotor–bearing–foundation system, the self-excited vibration of the oil film force between the bearing and the journal may cause the film to collapse. Under certain conditions, vibration will increase suddenly at that position and spread over the whole system in short time, which will cause strong vibration. In addition, the difference between the whirl frequency and the rotating frequency will cause alternating stress in the rotor, which may cause more severe harm to the rotor system than the synchronous vibration caused by unbalance does. As an important engineering problem, oil whirl often happens in practice. The main frequency feature of oil whirl is the increasing of 1/2X component.

Oil whirl can be obtained artificially by injecting oil evenly into the journal bearing at the end of the rotor, as shown in Figure 9.

Figure 10 shows a set of horizontal vibration data sampled at oil whirl condition. The sampling speed is 1·6 Hz, and the rotating speed is 3000 r.p.m.

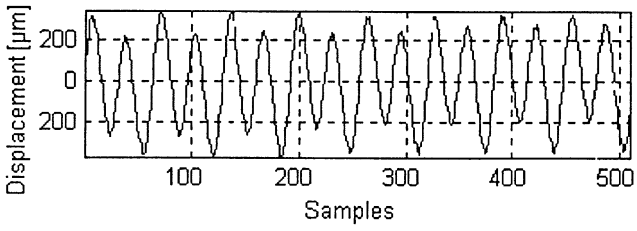

Figure 10. Oil whirl signal.

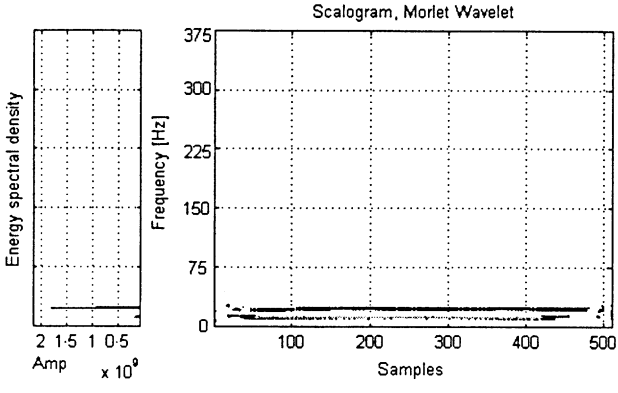

Figure 11. Spectrum and scalogram of oil whirl signal.

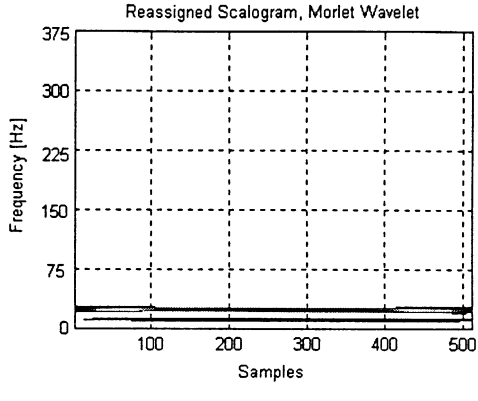

Figure 12. Reassigned scalogram of oil whirl signal.

The left side of Figure 11 is the spectrum of the oil whirl signal, in which 1/2X component can be recognized and is a special feature for oil whirl. However, compared with 1X component, the 1/2X is very small and will be overlooked easily. On the contrary, the 1/2X can be seen easily in the scalogram (the right side of Figure 11), and especially clearly on the reassigned scalogram (Figure 12). The results testify once again that the scalogram and the reassigned scalogram can give better description than the spectrum in extracting fault features at the early developing stage.

6.3. COUPLING MISALIGNMENT

Coupling misalignment, one of the most familiar faults, often denotes the slant or misalignment between the axes of two nearly rotors. When misalignment exists, a series of dynamic responses undesired will occur in the rotor system, such as coupling deflection, bearing abrasion and oil collapsing, etc. So it is very important to find misalignment as early as possible for ensuring the safe running of the machines. The main frequency feature of the coupling misalignment is the increase of 2X component.

Through the adjustment of the coupling, coupling misalignment can be manually simulated, as shown in Figure 13.

Figure 14 shows a set of horizontal vibration data sampled at coupling misalignment condition. The sampling speed is 1·6 Hz, and the rotating speed is 3000 r.p.m.

The spectrum, scalogram and reassigned scalogram of coupling misalignment signals are given in Figures 15 and 16. 2X component, which is the spectrum feature of the coupling misalignment, can be seen on all three figures. But in the order of distinctness, the reassigned scalogram is the best, then the scalogram and lastly the spectrum. The order is just that of quality of the three methods in extracting fault features.

7. ACTUAL MEASUREMENT SIGNAL ANALYSIS

In this section, the scalogram and the reassigned scalogram are used to analyze vibration data of an industrial machine. The machine is Guangzhou (in Southern China) 300 MW Pumped Storage Power Generator Unit (PSPGU). Its primary parameters are as follows: operating speed: 500 r.p.m., rated power: 306 MW, weight of the rotor: 600 t. The inner diameter of the stator and the outer diameter of the rotor are 4400 and 4311 mm respectively. The diameter of the shaft is 1000 mm. The PSPGU needs to run at several operating conditions, and is affected by many factors, such as hydraulic factors and electric factors. Therefore, the vibration is much more complex. The vibration signal of the start-up process is very complex, and has a strong non-stationary character and abundant frequency

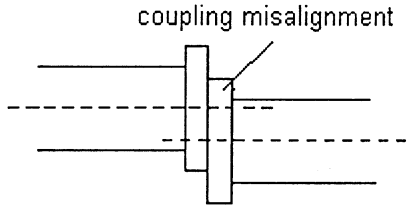

Figure 13. Simulating coupling misalignment.

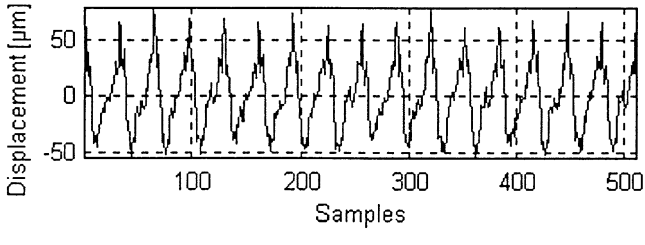

Figure 14. Coupling misalignment signal.

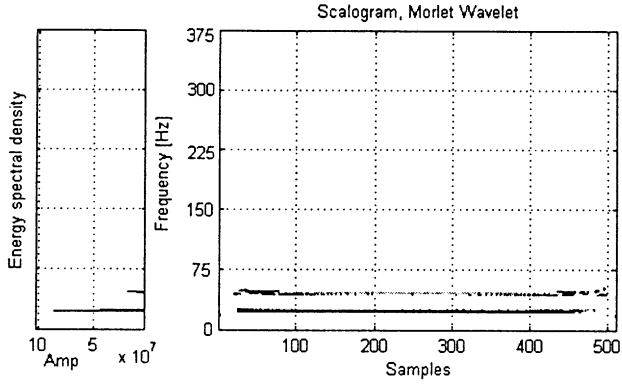

Figure 15. Spectrum and scalogram of coupling misalignment signal.

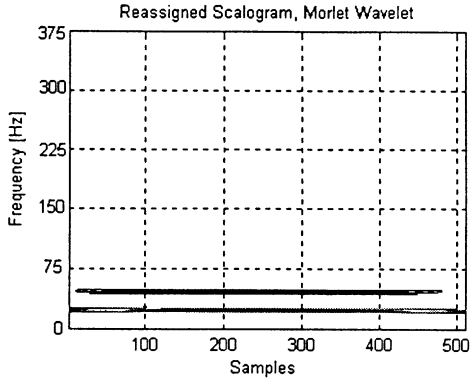

Figure 16. Reassigned scalogram of coupling misalignment signal.

components. So spectrum analysis is not enough to satisfy the request of analyzing the running condition of the machine. A way to obtain as much information as possible from the vibration signal is very important for evaluating the running condition of the unit. Figure 17 shows a set of vibration data at the position of the upper guide X that was sampled at the start-up process of generating mode through the PSTA-I monitoring system developed by Tsinghua University.

Though the data was sampled during the start-up process of the generating mode, the sampling time of a data set is very short. During this period, the change of rotating speed is very small and the rotating speed can thus be approximately regarded as constant. The rotating speed is corresponding to the 1X frequency of the spectrum (the left side of Figure 18). It can be seen from the spectrum that the energy of the signal concentrates mainly at the 1X component denoted by ① and its side frequency components, such as the component of ②. The 2X component denoted by ③ can be recognized, but its energy is low, and will be overlooked easily. The spectrum is able to show which frequency components the signal contains, but, unfortunately, the spectrum is unable to show the time distribution of components of the signal. The right-hand side of Figure 18 is the scalogram. Obviously, there are interference terms in the scalogram because the scalogram's concentration is not good and some components of the signal are very close, such as components ① and ②. But all components and their time of appearance can be approximately recognized through the scalogram. Figure 19 shows the reassigned scalogram. Obviously, the interference terms are

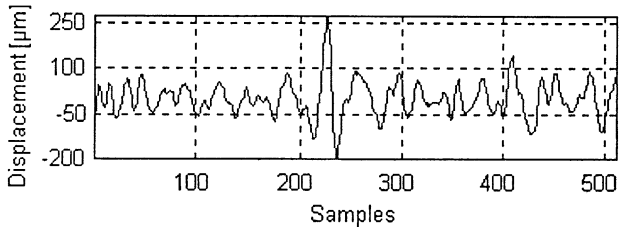

Figure 17. Vibration signal of the upper guide X.

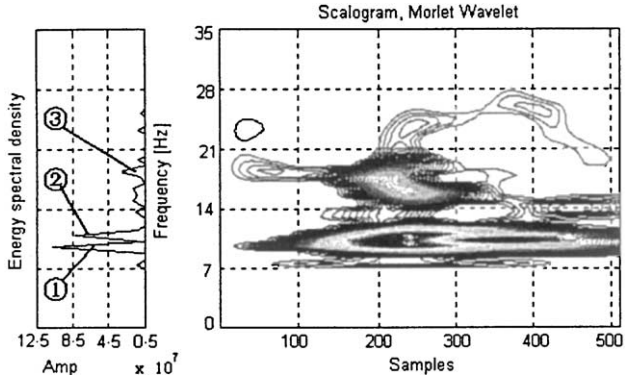

Figure 18. Spectrum and scalogram of vibration signal of the upper guide X. ① 1X component; ② a significant side frequency component; ③ 2X component.

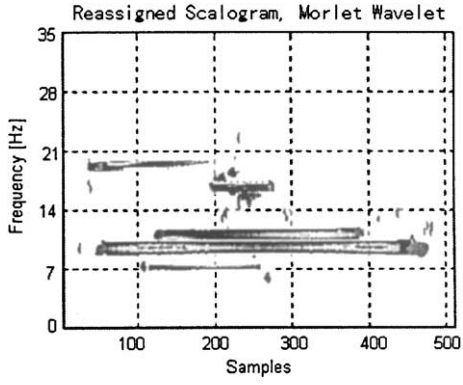

Figure 19. Reassigned scalogram of vibration signal of the upper guide X.

reduced in the reassigned scalogram, and some components, which are close to each other, can be discerned. For example, frequencies of components ① and ② are very close, but they can be discriminated easily through the reassigned scalogram. Furthermore, time distributions of some significant frequency components, such as ①, ② and ③, are shown clearly. It does testify that the reassigned scalogram can reveal the time–frequency characteristics of a signal and can give more useful information about a machine. All of these have shown the advantages of the reassigned scalogram in the time–frequency analysis.

8. CONCLUSIONS

In this paper, the wavelet scalogram and the reassigned scalogram have been used to analyze vibration signals, including numerical simulation signal, experimental data for three kinds of faults: rotor-to-stator rub-impact, oil whirl, coupling misalignment, all of which are typical faults of rotating machines, and the actual measurement data from a Pumped Storage Power Generator Unit. Comparison was carried out among the analysis results of the spectrum, scalogram and reassigned scalogram. The comparison results indicate that (1) the FFT spectrums are unable to reveal time–frequency characters of the signal, which make spectrums not suitable for the analysis of non-stationary signals. They are also unable to show components with low energy clearly, which makes spectrum unable to extract fault features at its early developing stage. (2) The scalogram as a useful time–frequency tool is suitable to non-stationary signal analysis, through which the time–frequency features of signals can be obtained. But the scalogram is unable to obtain good time and spectral concentration together in the time–frequency plane owing to the limitation of the Heisenberg–Gabor inequality, and at some conditions, interference terms will appear on the scalogram. (3) The reassigned scalogram has both good time and frequency concentration and few misleading interference terms, which makes the reassigned scalogram able to highlight the components with low energy and therefore be used to extract the fault features when the fault is at an early developing stage. In addition, both the scalogram and the reassigned scalogram can reflect the time–frequency character of the signal. Therefore, they are suitable to analyze non-stationary signals. In conclusion, the reassigned scalogram is a very effective method of vibration signal analysis for fault diagnostics of rotating machinery.

ACKNOWLEDGMENTS

This research is supported by a project (No. PD9521908Z2) from the Ministry of Science and Technology and a Visiting Fellowship provided to the second author by the State Key Laboratory of Vibration, Shock and Noise at Shanghai Jiao Tong University. Thanks are also due to the anonymous referees for their help in improving the English language.

REFERENCES

1. M. C. PAN and P. SAS 1996 *IEEE Proceedings of International Conference on Signal Processing* **2**, 1723–1726. Transient analysis on machinery condition monitoring.
2. P. C. RUSSELL, J. COSGRAVE, D. TOMTSIS, A. VOURDAS, L. STERGIOULAS and G. R. JONES 1998 *Measurement Science & Technology* **9**, 1282–1290. Extraction of information from acoustic vibration signals using Gabor Transform type devices.
3. I. S. KOO and W. W. KIM 2000 *ISA Transactions* **39**, 309–316. Development of reactor coolant pump vibration monitoring and a diagnostic system in the nuclear power plant.
4. G. T. ZHENG and P. D. MCFADDEN 1999 *Transactions of the American Society of Mechanical Engineers, Journal of Vibration and Acoustics* **121**, 328–333. A time–frequency distribution for analysis of signals with transient components and its application to vibration analysis.
5. L. A. WONG, J. C. CHEN 2001 *International Journal of Non-Linear Mechanics* **36**, 221–235. Nonlinear and chaotic behavior of structural system investigated by wavelet transform techniques.
6. Z. CHEN and Y. LU 1997 *Journal of Vibration Engineering* **10**, 147–155. Signal singularity detection and its application (in Chinese).
7. N. TANDON and A. CHOUDHURY 1999 *Tribology International* **32**, 469–480. Review of vibration and acoustic measurement methods for the detection of defects in rolling element bearings.

8. J. LIN and L. QU 2000 *Journal of Sound and Vibration* **234**, 135–148. Feature extraction based on Morlet wavelet and its application for mechanical fault diagnosis.
9. S. T. LIN and P. D. MCFADDEN 1997 *Mechanical Systems and Signal Processing* **11**, 603–609. Gear vibration analysis by B-spline wavelet-based linear transform.
10. F. AUGER and P. FLANDRIN 1995 *IEEE Transactions on Signal Processing* **43**, 1068–1089. Improving the readability of time–frequency and time-scale representations by the reassignment method.
11. K. KODERA, R. GENDRIN and C. DE VILLEDARY 1986 *IEEE Transactions on Acoustics, Speech, Signal Processing* **ASSP-34**, 64–76. Analysis of time-varying signals with small BT values.
12. P. FLANDRIN, C.-M. ERIC and A. PATRICE 1995 *Proceedings of SPIE* **2569**, 152–163. Reassigned scalograms and their fast algorithms.
13. B. WEN, J. GU, S. XIA and Z. WANG 2000 *Advanced Rotor Dynamics—Theory, Technique and Application*. Beijing: Mechanical Industry Press (in Chinese).
14. F. CHU and Z. ZHANG 1998 *Journal of Sound and Vibration* **210**, 1–18. Bifurcation and chaos in a rub-impact Jeffcott rotor system.